## PAPER

CrossMark
click for updates

# New roles for metal–organic frameworks: fuels for environmentally friendly composites†

Hui Su,[a] Jichuan Zhang,[a] Yao Du,[a] Pengcheng Zhang,[a] Shenghua Li,*[a] Tao Fang[b] and Siping Pang*[a]

Composite energetic materials are widely used in mining, air bag modules and propellants, and welding because they can release a large amount of stored energy on combustion. Unfortunately, common composite formulations exhibit incomplete combustion of these agents and their toxic components, reducing the yield and causing emission of harmful gaseous products. We report a new type of formulation using an energetic metal–organic framework, $[Cu(atrz)_3(NO_3)_2]_n$ (atrz = 4,4'-azo-1,2,4-triazole), as an active component. Its physicochemical properties such as the decomposition temperature, heat of reaction, sensitivity, and gas generation rate were measured. Compared with traditional composites, these composites exhibit superior characteristics such as low toxicity, high peak pressure, insensitivity, and high activity, and they produce very little solid residue. In light of their excellent properties, they exhibit potential as green gas generators for future applications and open up a new field for the application of MOFs.

## Introduction

Energetic materials are widely used[1–5] in micropropulsion, mining, air bag modules, ammunition primers, and propellants because they produce large amounts of hyperthermal gas products. With increasing awareness of environmental and ecological concerns, much effort[6–10] has been given to seeking next-generation green composites with suitable compositions that not only have excellent properties to meet the requirements of their wide range of applications, but also avoid deleterious components and elements to meet environmental protection requirements.

Composite energetic materials are mixtures of a fuel (*e.g.*, aluminum particles) and oxidizing materials (*e.g.*, $Fe_2O_3$, CuO, $MoO_3$),[11,12] and the energy of the gas products generated depends on the enthalpy of reaction, which arises from the oxidation–reduction reaction between the fuel and oxidizer. Although these materials usually have a much higher energy density[13] than organic explosives (*e.g.*, TNT, nitrocellulose, RDX), their generated energies are lower than the theoretical values because a large portion of the fuel powders is usually unreacted owing to the low reaction rates between the fuel and oxidizer and the slow mass transfer rate between the reactants. More importantly, these unreacted powders are serious pollutants[14] that are an important

source of PM 2.5 owing to their size distribution and the difficulty of decomposing them. More recently, many other more powerful molecules have been introduced into formulations for their high energy content and strong activity. Many of them are typically composed of salts ($NaN_3$,[15] $NH_4ClO_4$,[12] and $KClO_4$ (ref. 12)). These molecules display very promising gas-generating behavior; however, they would induce serious environmental pollution[16,17] during manufacture, transport, and application. In practice, sodium azide has been confirmed as a deadly poison,[18] and perchlorate has a very large negative impact on human health as well as the ozone layer, because as much as 98% of the available chlorine ions may be converted to HCl gas[16,17,19] when perchlorate is used in common composite propellant formulations. A recent report introduced periodate ($NaIO_4$, $KIO_4$) salts[13,20] as oxidizers because of their low toxicity; however, the resulting composites have relatively low peak pressures or full width at half-maximum (FWHM) burn times,[13] limiting their ability to provide gaseous products. These inadequacies may be due to the shortage of gaseous elements (*e.g.*, CHON elements) in the formulation and the presence of iodine elements with a very large atomic mass (126.9), which decreases the amount of gaseous products and degrades the performance of the composites. The fabrication of high-performance environmentally friendly energetic materials and their application as green gas generators remain challenging.

Metal–organic frameworks (MOFs) are a new class of porous materials and have attracted great attention because of their fascinating molecular structures and extensive applications in catalysis,[21,22] gas storage,[23] and chemical sensors.[24] Energetic MOFs,[10,25–27] an important type of such porous materials, use mainly azole heterocycles and their derivatives as ligands.

*[a]School of Materials Science & Engineering, Beijing Institute of Technology, Beijing 100081, PR China. E-mail: lishenghua@bit.edu.cn; pangsp@bit.edu.cn*

*[b]Beijing Institute of Aerospace Testing Technology, Beijing 100074, PR China*

† Electronic supplementary information (ESI) available. See DOI: 10.1039/c6ra28679h

Significantly, the combustion products of these nitrogen-rich ligands are innoxious, produce less smoke, and are environmentally friendly. Energetic MOFs are a unique class owing to their interesting structures, their high-energy-density ligands,[8,10] and the resulting fascinating structural motifs that appear at the high heat of detonation, which demonstrate their potential as fuels. Moreover, because of their porous structure, MOFS may produce two-phase flow[28–30] and enhance the reaction between the gas flow and unburned porous solids, which supports convective transport and thus affects the performance of these composites. Moreover, the components of energetic MOFs contain large amounts of gaseous elements (*e.g.*, CHON elements), making them favorable for the generation of gaseous products during combustion. Accordingly, energetic MOFs are ideal fuels because of their environmentally friendly combustion products, high heats of detonation, and special molecular structures. Although many energetic MOFs have been synthesized[31–33] in the past few years, the exploration of MOFs in composite energetic materials has not been reported.

Here, we report a novel type of composite energetic materials based on a powerful three-dimensional energetic MOF, $[Cu(atrz)_3(NO_3)_2]_n$ [MOF(Cu), atrz = 4,4'-azo-1,2,4-triazole]. We chose to use MOF(Cu)[34] as the fuel for the following reasons: (1) it possesses a superhigh heat of detonation and a high nitrogen content (53.35%), which could improve the gas-generating performance; (2) it has a porous structure, so it supports convective transport[28–30] and may promote complete combustion; (3) because of its high nitrogen content, its combustion products are innoxious, contain less smoke, and are more environmentally friendly, so MOF(Cu) satisfies the demand for green material development. In addition, periodate salts were selected as the oxidizer because of their low toxicity and high oxygen content. Their physicochemical properties such as the decomposition temperature, heat of reaction, and gas-generating performance were measured, and the results demonstrated their potential as green composite energetic materials in future applications.

# Experimental

### Chemicals and materials

$NaIO_4$ and $KIO_4$ were purchased from Aladdin Corporation and used without further purification. Copper oxide (CuO, 50 nm) was purchased from Sigma-Aldrich Corporation, and aluminum (Al, 50 nm) nanopowders were purchased from Beijing DK Nano Technology Co. Ltd. The purity of the aluminum nanoparticle was 80%, according to the manufacturer's data, and was further confirmed by thermogravimetric and differential scanning calorimetry (DSC) measurement (Fig. S1†).

### Preparation of MOF(Cu)

According to a literature procedure,[34] green energetic MOF(Cu) was prepared by a hydrothermal method. Yield: 81%. Elemental analysis (%) calculated for C, 21.20; H, 1.78; N, 53.56. Found: C, 21.02; H, 1.81; N, 53.41. Infra-red spectrum (IR, KBr pellets, $\lambda$, cm$^{-1}$): 3118, 1504, 1395, 1356, 1187, 1041, 886, 627. Powder X-ray diffraction (PXRD, Fig. S2†), IR (Fig. 2), and elemental

analyses confirmed that the structure of the as-prepared samples was consistent with that reported for MOF(Cu).

### Preparation of the energetic composites

$NaIO_4$ or $KIO_4$ was stoichiometrically mixed with MOF(Cu). Approximately 10 mL of hexane was then added to each mixture, and the mixtures were ultrasonicated for 30 min to ensure thorough mixing. The hexane was allowed to evaporate in air, and then the samples were placed in vacuum at 60 °C for 12 h to remove any remaining hexane and moisture. The powder was very easily broken with a spatula until the consistency of each sample was that of a loose powder. The MOF(Cu)/NaIO$_4$ composite contained 33.4% MOF(Cu) and 66.6% NaIO$_4$. The MOF(Cu)/KIO$_4$ composite contained 31.8% MOF(Cu) and 68.2% KIO$_4$. The composite Al/CuO (Al, ~0.050 μm; CuO, ~0.050 μm) was used as a reference, and it contained 22% Al and 78% CuO.

### Measurement of heat of reaction and ignition temperature using differential scanning calorimetry measurement/thermogravimetric

In this paper, a TG-DSC Q2000 differential scanning calorimeter was employed to determine the ignition temperatures, heats of reaction and compatibility of thermites. About 1.5 mg of sample was used and the temperature was programmed to 1000 °C (1273 K) at the rate of 10 °C min$^{-1}$ in 60 mL min$^{-1}$ N$_2$ flow. A minimum of three measurements were taken for each composites under identical experimental conditions to quantify the error. The ignition temperature was usually regarded as the onset temperature of an exothermic reaction and also as the lowest temperature that can induce the thermal explosion of a sample. The heat of reaction was obtained by the integration of the exothermic peaks.

### Measurement of sensitivity

The impact sensitivity was tested on a type 12 tooling according to "up and down" method (Bruceton method). A 2.5 kg weight was dropped from a set height onto a 20 mg sample placed on 150 grit garnet sandpaper. Each subsequent test was made at the next lower height if explosion occurred and at the next higher height if no explosion happened. 50 drops were made from different heights, and an explosion or non-explosion was recorded to determine the results. RDX was considered as a reference compound, and the impact sensitivity of RDX is 7.4 J.[26]

The friction sensitivity was tested on a FSKM-10 BAM friction apparatus. RDX was also used as a reference compound, and its friction sensitivity is 110 N.[26]

The electrostatic sensitivity was tested on a FSKM 50/20K apparatus produced by OZM Research. Typically a 25 mg sample was placed between the porcelain plate and peg. The weight of leading at least one ignition in six times was recorded. The friction sensitivity of RDX is 0.2 J.[26] Test conditions: 25 °C (temperature); 34% (relative humidity).

### High-speed imaging

The high speed digital imaging of sample combustion was taken at a resolution of 500 × 500 and frame rate of 5000 fps (200 μs per

frame) by an Optronis CR3000x2 high-speeding camera. The high speed imaging experiment was conducted in air at atmospheric pressure. Typically a 25 mg sample was loaded in a crucible for the measurement and ignited by joule heating of a nichrome coil on top of the loose powder.

### Combustion cell characterization

A constant volume combustion cell ($\sim$13 cm$^3$) was used to simultaneously measure the pressure rise[12,13] of the composite (Fig. S4†). In this study, 25.0 mg of sample was placed inside the combustion cell and ignited by joule heating of a nichrome coil on top of the loose powder. Other composite samples (control experiments) were also tested in combustion cell for comparison purpose.

## Results and discussion

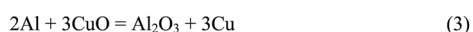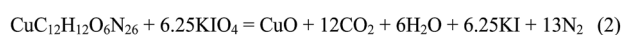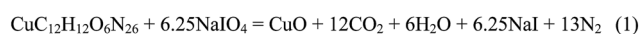### Fabrication and characterization of composite energetic materials

According to a literature procedure,[34] green energetic MOF(Cu) was prepared from a hydrothermal reaction of 4,4′-azo-1,2,4-triazole (atrz) with Cu(NO$_3$)$_2$ at 100 °C; this material can be synthesized with high yield and purity. The PXRD patterns (Fig. S2†) showed that the framework of MOF(Cu) was well maintained even after it was heated at 200 °C for 24 h in air, confirming that it is highly stable.

The composites were prepared by ultrasonically mixing MOF(Cu) with a periodate oxidizer (NaIO$_4$ or KIO$_4$) in a stoichiometric ratio, as shown in Scheme 1 [eqn (1) and (2)], and an Al/CuO composite[13] (Al, $\sim$0.050 μm; CuO, $\sim$0.050 μm) was used as a reference material [eqn (3)] to demonstrate the reliability of the present method.

The MOF(Cu)-based composites ranged in size from 10 to 30 μm according to scanning electron microscopy (SEM) images (Fig. 2 and S5†). Energy-dispersive X-ray spectroscopy (EDS) elemental maps (Fig. 2) of the MOF(Cu)-based composites showed that the MOF(Cu) particles and oxidizer particles were relatively evenly distributed. In addition, the composites were further examined by PXRD and IR analyses (Fig. 1). The PXRD patterns showed that many main peaks of MOF(Cu) still appeared after the formation of the MOF(Cu)/NaIO$_4$ and MOF(Cu)/KIO$_4$ composites, confirming that the structure of MOF(Cu) was well maintained. These main peaks of MOF(Cu) are marked with red circles or purple squares. In addition, according to the PDF card and IR analysis of the periodate salts, the MOF(Cu)-based composites also contained periodate salts.

### Initial safety testing

For the initial safety testing, the impact and friction sensitivity of MOF(Cu)/NaIO$_4$ and MOF(Cu)/KIO$_4$ were measured using
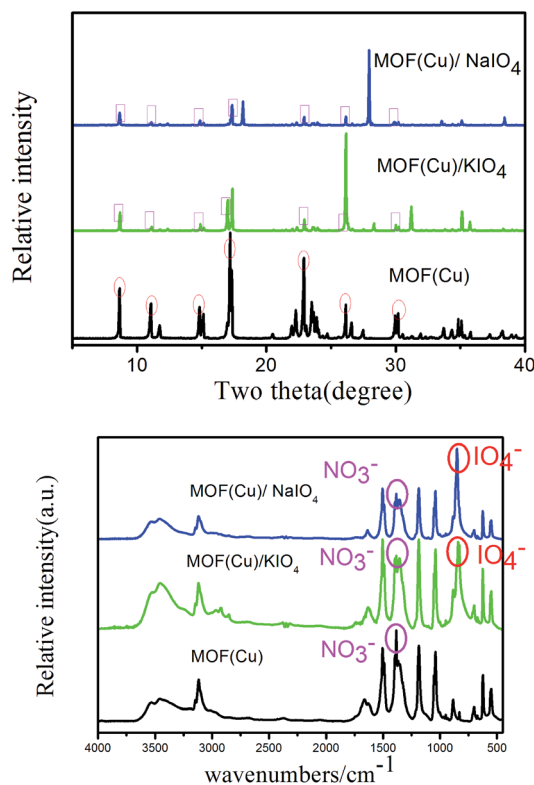


Fig. 1   PXRD and IR analyses for MOFs and MOF-based composites.

a standard BAM Fallhammer and a BAM friction tester, and the electrostatic discharge sensitivity was tested on an FSKM 50/20 apparatus. The results are summarized in Table 1. The impact sensitivities of MOF(Cu)/NaIO$_4$ and MOF(Cu)/KIO$_4$ are 10 and 9 J, respectively, which are lower than that of the Al/CuO nanocomposite (3 J). Although their impact sensitivities are lower than that of the corresponding aluminum-based counterparts, their friction sensitivities [MOF(Cu)/NaIO$_4$, 8 N; MOF(Cu)/KIO$_4$, 32 N] were similar to those of Al/NaIO$_4$ (6 N)[13] and AlKIO$_4$ (32 N),[13] respectively. All of the MOF(Cu)-based composites showed much lower sensitivity toward electrostatic discharge [MOF(Cu)/NaIO$_4$, 0.19 J; MOF(Cu)/KIO$_4$, 0.13 J]. Note that when compared with other traditional composites (Al/NaIO$_4$, <0.0084 J; Al/KIO$_4$, <0.0084 J),[13] the MOF(Cu)-based composites [MOF(Cu)/NaIO$_4$, 0.13 J; MOF(Cu)/KIO$_4$, <0.19 J] exhibited superior performance,

$$CuC_{12}H_{12}O_6N_{26} + 6.25NaIO_4 = CuO + 12CO_2 + 6H_2O + 6.25NaI + 13N_2 \quad (1)$$

$$CuC_{12}H_{12}O_6N_{26} + 6.25KIO_4 = CuO + 12CO_2 + 6H_2O + 6.25KI + 13N_2 \quad (2)$$

$$2Al + 3CuO = Al_2O_3 + 3Cu \quad (3)$$

Scheme 1   Reaction equations of MOFs-based composites and reference material.

Table 1   Physicochemical properties of different composite

| Entry | $T_d{}^a$ | Heat$^b$ | IS$^c$ | FS$^d$ | ESD$^e$ | $P_{max}{}^f$ | $T^g$ |
|---|---|---|---|---|---|---|---|
| MOF(Cu)–NaIO$_4$ | 232 | 2.63 | 10 | 8 | 0.13 | 1.96 | 28.7 |
| MOF(Cu)–KIO$_4$ | 227 | 2.053 | 9 | 32 | 0.19 | 1.79 | 19.4 |
| Al–CuO(nano) | 767$^h$ | 3.79 | 3 | <6 | <0.008$^h$ | 0.6$^h$ | 0.170$^h$ |
| Al–NaIO$_4$(nano)$^h$ | 607 | — | — | <6 | <0.0084 | 4.0 | 0.124 |
| Al–KIO$_4$(nano)$^h$ | 677 | — | — | 32 | <0.0084 | 3.8 | 0.124 |

$^a$ Decomposition temperature (DSC, °C). $^b$ The actual measurement (kJ g$^{-1}$). $^c$ Impact sensitivity (J). $^d$ Friction sensitivity (N). $^e$ Electrostatic sensitivity (J). $^f$ The peak pressures (MPa). $^g$ Full width at half maximum (ms). $^h$ Ref. 13.
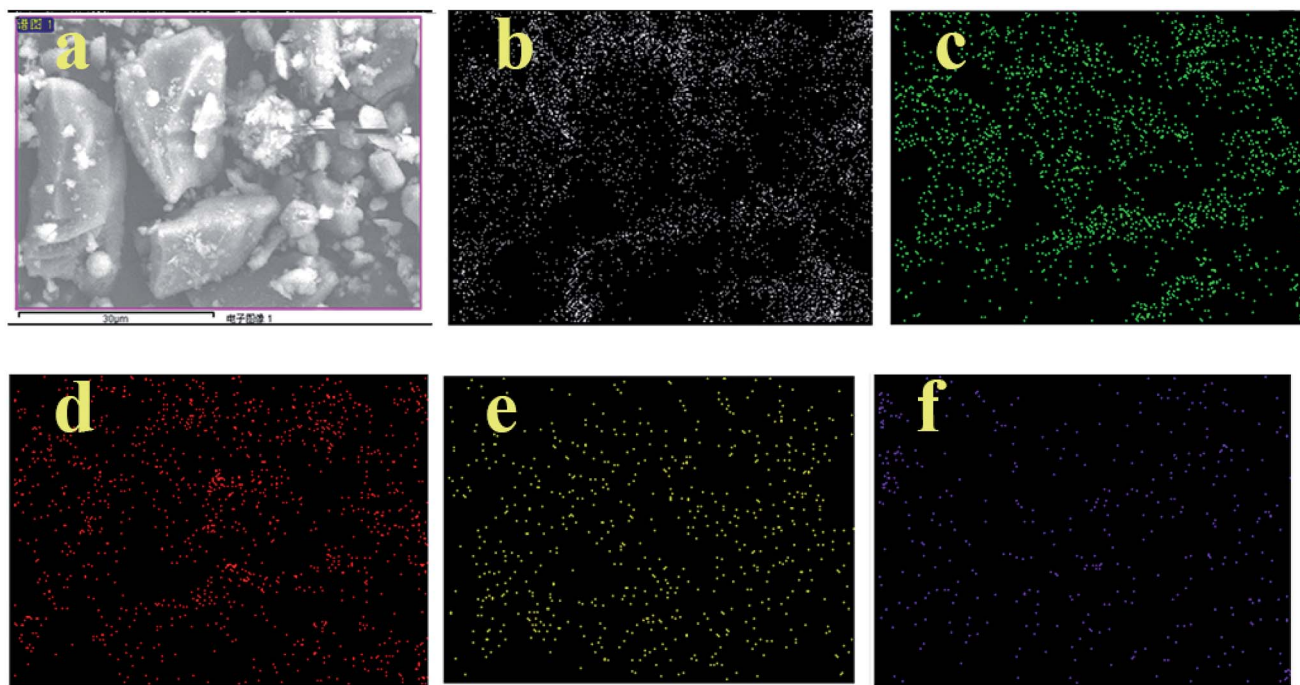
**Fig. 2** SEM images and EDS elemental maps of the MOF(Cu)/NaIO$_4$ composite: (a) SEM images; (b) C (white); (c) N (blue); (d) O (red); (e) Cu (yellow); (f) I (purple).
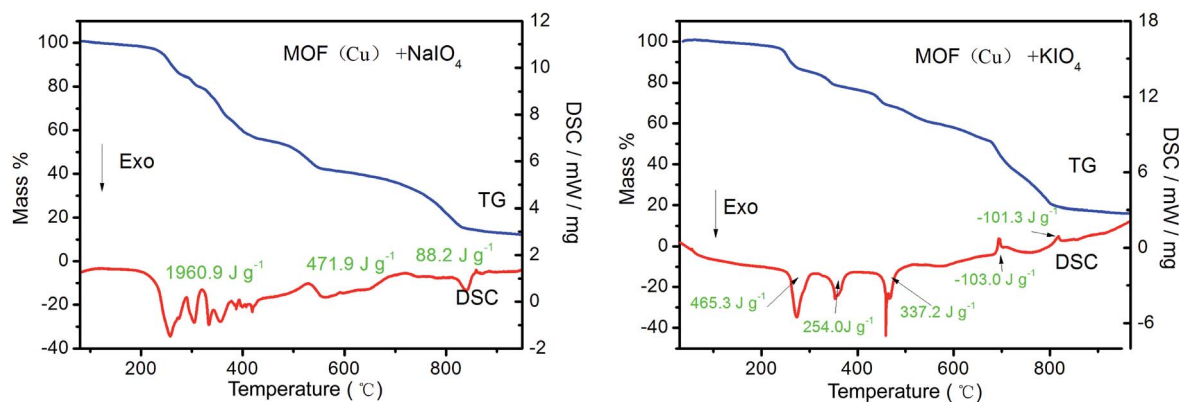


**Fig. 3** DSC/TG curves of MOF-based composites. The heats of reaction are obtained by the integration of the exotherm peaks.

indicating a comparable margin of safety when handling them (the human body can generate up to 0.025 J of static electricity[35]). The relatively low sensitivity may arise from the high stability and insensitivity of energetic MOF(Cu), and low sensitivity is important for safe manufacture, transport, and application. This point has also been previously confirmed by Yang.[36]

### Thermodynamic study

In addition to the sensitivity, the ignition temperature is also an important property of a composite and is strongly related to its safe delivery, storage, and application. Many previous studies have used DSC to determine the ignition temperature of conventional composites. In a DSC curve, the ignition temperature is usually regarded as the lowest temperature that can

induce spontaneous exothermic reaction of a sample. From the DSC curves (Fig. 3), the ignition temperatures of MOF(Cu)/NaIO$_4$ and MOF(Cu)/KIO$_4$ are only 232 °C and 227 °C, respectively, which are lower than those of common composites (for example, >1227 °C for Al/Fe$_2$O$_3$,[12] 822 °C for Al/(Fe$_2$O$_3$ + KClO$_4$),[12] 767 °C for Al/CuO,[13] 607 °C for Al/NaIO$_4$,[13] and 677 °C for Al/KIO$_4$ (ref. 13)). Their remarkably low ignition temperatures are attributed to the high activity and porous structure of MOF(Cu). The high activity reduces the thermal energy required to initiate reactivity, and the porous structure may enhance the reaction between the gas flow and unburned porous solids, reducing the need for a thermal stimulus.

The enthalpies of combustion of gram-scale MOF-based composites and the reference material were measured using

an oxygen bomb calorimeter. The measured heats of reaction for MOF(Cu)/NaIO$_4$ and MOF(Cu)/KIO$_4$ are 2.63 and 2.05 kJ g$^{-1}$, respectively, whereas that of the reference material, Al/CuO, is 3.79 kJ g$^{-1}$, which is similar to its theoretical value (3.9 kJ g$^{-1}$),[1] demonstrating the reliability of the proposed method. We also confirmed that these samples, like other samples of aluminum-based composite materials containing perchlorate nano-particles, were hard to ignite or exhibited incomplete combustion under low tension and low mass.[37–39] The experimental results for MOF(Cu)/KIO$_4$ agree well with this theory. The heat

of reaction (2.63 kJ g$^{-1}$) for MOF(Cu)/NaIO$_4$, unlike those of most composite materials, is similar to the value calculated using the single exothermic peak area (2.44 kJ g$^{-1}$), possibly because of the approximate initial decomposition temperatures (Fig. S3†) of MOF(Cu) (269 °C) and NaIO$_4$ (290 °C), which presumably are the result of the good compatibility between MOF(Cu) and NaIO$_4$. In addition, the heat of reaction of MOF(Cu)/NaIO$_4$ (2.63 kJ g$^{-1}$; (DSC) calculation value) is higher than or approximately equal to that of the majority of aluminum-based composites, including Al/CuO (1.2 kJ g$^{-1}$),[40] Al/WO$_3$ (1.17 kJ g$^{-1}$),[41] Al/Co$_3$O$_4$ (2.50 kJ g$^{-1}$),[42] and Al/Fe$_2$O$_3$ (2.83 kJ g$^{-1}$).[43] The relatively high heat of reaction of MOF(Cu)/NaIO$_4$ could result from the good compatibility between MOF(Cu) and NaIO$_4$, which facilitates complete combustion and produces environmentally friendly combustion products.

## Combustion performance

To explore the reactivity of the MOF(Cu)-based composites, a fixed mass (25 mg) of each sample in a loose powder was ignited in each shot, and the pressure signals of the combustion cell (~13 cm$^2$) due to burning were measured (Fig. 4). All the systems showed a fast pressure rise, on the order of microseconds. The peak pressures are 1.96 and 1.79 MPa for MOF(Cu)/NaIO$_4$ and MOF(Cu)/KIO$_4$, respectively, which are significantly better than that of the reference material, Al/CuO, which is only 0.55 MPa (its literature value[13] is 0.6 MPa, and its measured
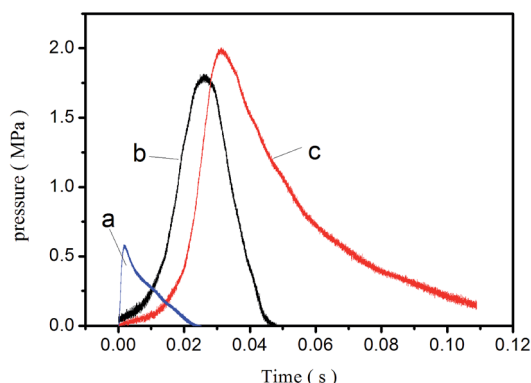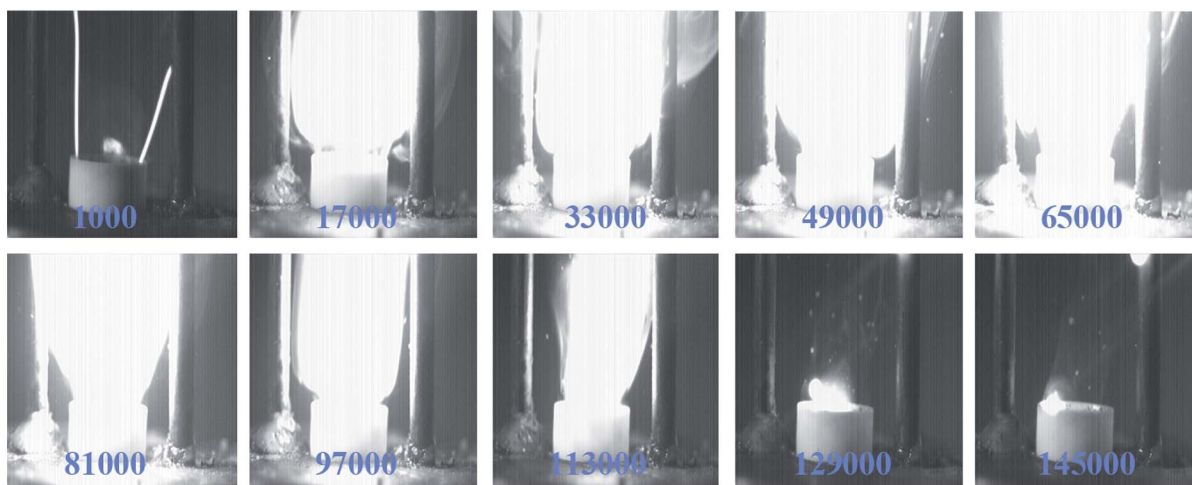


Fig. 4 Pressure *versus* time for the MOF(Cu)-based composite and the reference samples s: (a) Al/CuO; (b) MOF(Cu)/KIO$_4$; (c) MOF(Cu)/NaIO$_4$.
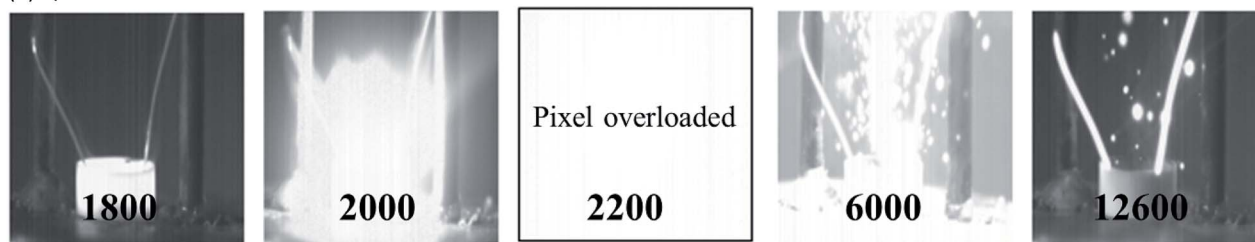


Fig. 5 Visualization of combustion of MOF(Cu)/NaIO$_4$ (a) and Al/CuO (b) composite, as captured by high-speeding camera. The labeled numbers are time elapsed (μs) after triggering.

value is very similar, demonstrating the reliability of our test method). The peak pressures of MOF(Cu)/NaIO$_4$ and MOF(Cu)/KIO$_4$ are slightly higher than that of Al/CuO, possibly because MOF(Cu) contains large amounts of gaseous elements (e.g., CHON elements) and releases a large amount of gaseous products upon reaction.

More importantly, MOF(Cu)/NaIO$_4$ (28.7 ms) and MOF(Cu)/KIO$_4$ (19.4 ms) exhibit remarkable FWHM burn times that far exceed those of Al/CuO, 0.280 ms (0.170 ms (ref. 13)), Al/NaIO$_4$ (0.124 ms),[13] and Al/KIO$_4$ (0.124 ms).[13] The relatively high peak pressures and long FWHM burn times could result from the composites' high content of gaseous elements (e.g., CHON elements), which would release a massive amount of gases (e.g., N$_2$, CO$_2$), and the special three-dimensionally ordered macroporous structure, which supports convective transport[28–30] of high-temperature gas products to unburned solids and thus promotes complete reactions.

In addition, the ratio of the solid residue mass to the sample mass of MOF(Cu)/NaIO$_4$ is only 6.8%, very likely because MOF(Cu) has a high nitrogen content (53.35%), and the ratio of the solid residue mass to the sample mass of NaIO$_4$ is less than 20%. Moreover, most composite energetic materials with the lack of gas elements (e.g., CHON elements) usually produce a large quantity (e.g., Al/Fe$_2$O$_3$; almost 100%) of solid residue during combustion, which would inevitably cause environmental pollution.[14] In contrast, MOF(Cu)/NaIO$_4$ leaves very little solid residue after combustion, and the results further suggest that MOF(Cu)-based composites are suitable for use as gas generators.

To test the utility of the MOF(Cu)-based composites, we also performed high-speed imaging of 25 mg samples in a crucible, which showed a violent flame front (Fig. 5) similar to that observed for the Al/CuO composite (Fig. S6†). However, the MOF(Cu)-based composites showed a longer burning time MOF(Cu)/NaIO$_4$, 144 ms; Al/CuO, <10.6 ms, which facilitates the production of a sustained impulsive force. In short, the relatively high peak pressures, long FWHM burn time, very little solid residue after combustion, and environmental friendliness of the combustion products illustrated their potential for green gas-generation in future applications.

## Conclusions

We demonstrated a novel type of environmentally friendly composite based on energetic MOFs as a fuel. Compared with common composites, the new formulations exhibit desirable characteristics such as low toxicity, low sensitivity, and high activity, and they produce very little solid residue. Among them, the measured heat of reaction, ignition temperature, FWHM burn time, and peak pressure for MOF(Cu)/NaIO$_4$ were 2.63 kJ g$^{-1}$, 232 °C, 28.7 ms, and 1.96 MPa, respectively. Considering all of its excellent properties, it exhibits potential as a green secondary gas generator in future applications and opens a new field for the application of MOFs.

## Conflict of interest

The authors declare no competing financial interest.

## Acknowledgements

## Notes and references

1 S. J. Widdis, K. Asante, D. L. Hitt, M. W. Cross, W. J. Varhue and M. R. McDevitt, *IEEE ASME Trans. Mechatron.*, 2013, **18**, 1250–1258.

2 Q. Zou, B. Lin, C. Zheng, Z. Hao, C. Zhai, T. Liu, J. Liang, F. Yan, W. Yang and C. Zhu, *J. Nat. Gas Sci. Eng.*, 2015, **26**, 960–973.

3 E. M. Dorofeenko, D. B. Lempert and G. N. Nechiporenko, *Russ. J. Appl. Chem.*, 2011, **84**, 1229–1232.

4 X. Zhou, M. Torabi, J. Lu, R. Shen and K. Zhang, *ACS Appl. Mater. Interfaces*, 2014, **6**, 3058–3074.

5 V. A. Arkhipov and A. G. Korotkikh, *Combust. Flame*, 2012, **159**, 409–415.

6 T. M. Klapötke and G. Holl, *Green Chem.*, 2001, **3**, G75–G77.

7 A. Cohen, Y. Yang, Q. Yan, A. Shlomovich, N. Petrutik, L. Burstein, S. Pang and M. Gozin, *Chem. Mater.*, 2016, **28**, 6118–6126.

8 W. Gao, X. Liu, Z. Su, S. Zhang, Q. Yang, Q. Wei, S. Chen, G. Xie, X. Yang and S. Gao, *J. Mater. Chem. A*, 2014, **2**, 11958–11965.

9 Y. Wang, S. Li, Y. Li, R. Zhang, D. Wang and S. Pang, *J. Mater. Chem. A*, 2014, **2**, 20806–20813.

10 X. Liu, W. Gao, P. Sun, Z. Su, S. Chen, Q. Wei, G. Xie and S. Gao, *Green Chem.*, 2015, **17**, 831–836.

11 R. A. Yetter, G. A. Risha and S. F. Son, *Proc. Combust. Inst.*, 2009, **32**, 1819–1838.

12 C. Wu, K. Sullivan, S. Chowdhury, G. Jian, L. Zhou and M. R. Zachariah, *Adv. Funct. Mater.*, 2012, **22**, 78–85.

13 G. Jian, J. Feng, R. J. Jacob, G. C. Egan and M. R. Zachariah, *Angew. Chem.*, 2013, **125**, 9925–9928.

14 E. Vega, H. Ruiz, S. Escalona, A. Cervantes, D. Lopez-Veneroni, E. Gonzalez-Avalos and G. Sanchez-Reyna, *Atmos. Pollut. Res.*, 2011, **2**, 477–483.

15 S. B. Kim, K. J. Kim, M. H. Cho, J. H. Kim, K. T. Kim and S. H. Kim, *ACS Appl. Mater. Interfaces*, 2016, **8**, 9405–9412.

16 B. D. Andrea and F. Lillo, *J. Propul. Power*, 1999, **15**, 713–718.

17 D. Lempert, G. Nechiporenko, G. Dolganova and L. Stesik, *Chemical Physics Reports*, 1997, **16**, 1629–1641.

18 I. L. Blanc-Louvry, P. Laburthe-Tolra, V. Massol, F. Papin, J. P. Goulle, G. Lachatre, J. M. Gaulier and B. Proust, *Forensic Sci. Int.*, 2012, **221**, e17–e20.

19 B. C. Terry, T. R. Sippel, M. A. Pfeil, I. E. Gunduz and S. F. Son, *J. Hazard. Mater.*, 2016, **317**, 259–266.

20 J. D. Moretti, J. J. Sabatini and G. Chen, *Angew. Chem.*, 2012, **124**, 7087–7089.

21 D. T. Genna, A. G. Wong-Foy, A. J. Matzger and M. S. Sanford, *J. Am. Chem. Soc.*, 2013, **135**, 10586–10589.

22 Q. L. Zhu, J. Li and Q. Xu, *J. Am. Chem. Soc.*, 2013, **135**, 10210–10213.

23 N. L. Rosi, J. Eckert, M. Eddaoudi, D. T. Vodak, J. Kim, M. O. Keeffe and O. M. Yaghi, *Science*, 2003, **300**, 1127–1129.

24 M. P. Suh, H. J. Park, T. K. Prasad and D. W. Lim, *Chem. Rev.*, 2012, **112**, 782–835.

25 O. S. Bushuyev, P. Brown, A. Maiti, R. H. Gee, G. R. Peterson, B. L. Weeks and L. J. Hope-Weeks, *J. Am. Chem. Soc.*, 2012, **134**, 1422–1425.

26 J. Zhang, Y. Du, K. Dong, H. Su, S. Zhang, S. Li and S. Pang, *Chem. Mater.*, 2016, **28**, 1472–1480.

27 Y. X. Tang, C. L. He, L. A. Mitchell, D. A. Parrish and J. M. Shreeve, *Angew. Chem., Int. Ed.*, 2016, **55**, 5565–5567.

28 Y. He, R. Krishna and B. Chen, *Energy Environ. Sci.*, 2012, **5**, 9107–9120.

29 Q. Zhai, Q. Lin, T. Wu, L. Wang, S. Zheng, X. Bu and P. Feng, *Chem. Mater.*, 2012, **24**, 2624–2626.

30 H. B. Zhang, M. J. Zhang, P. Lin, V. Malgras, J. Tang, S. M. Alshehri, Y. Yamauchi, S. W. Du and J. Zhang, *Chem.–Eur. J.*, 2016, **22**, 1141–1145.

31 J. Zhang and J. M. Shreeve, *Dalton Trans.*, 2016, **45**, 2363–2368.

32 S. Zhang, Q. Yang, X. Liu, X. Qu, Q. Wei, G. Xie, S. Chen and S. Gao, *Coord. Chem. Rev.*, 2016, **307**, 292–312.

33 K. A. McDonald, S. Seth and A. J. Matzger, *Cryst. Growth Des.*, 2015, **15**, 5963–5972.

34 S. Li, Y. Wang, C. Qi, X. Zhao, J. Zhang, S. Zhang and S. Pang, *Angew. Chem.*, 2013, **125**, 14281–14285.

35 N. Fischer, D. Fischer, T. M. Klapötke, D. G. Piercey and J. Stierstorfer, *J. Mater. Chem.*, 2012, **22**, 20418–20422.

36 While the manuscript was under preparation, a new aluminum-based nanothermites was reported: X. Yang, X. Jiang, Y. Huang, Z. Guo and L. Shao, *ACS Appl. Mater. Interfaces*, 2017, DOI: 10.1021/acsami.6b15098.

37 V. A. Babuk, V. P. Belov and G. G. Shelukhin, *Combust., Explos. Shock Waves*, 1981, **17**, 264–268.

38 T. M. Klapötke, F. X. Steemann and M. Succecka, *Propellants, Explos., Pyrotech.*, 2013, **38**, 29–34.

39 Y. L. Zhu, H. Huang, H. Ren and Q. J. Jiao, *J. Korean Chem. Soc.*, 2013, **57**, 109–114.

40 M. Petrantoni, C. Rossi, L. Salvagnac, V. Conédéra, A. Estève and C. Tenaileau, *J. Appl. Phys.*, 2010, **108**, 084323.

41 Y. Wang, W. Jiang, Z. Cheng, W. Chen, C. An, X. Song and F. Li, *Thermochim. Acta*, 2007, **463**, 69–76.

42 D. Xu, Y. Yang, H. Cheng, Y. Li and K. Zhang, *Combust. Flame*, 2012, **159**, 2202–2209.

43 W. Zhang, B. Yin, R. Shen, J. Ye, J. A. Thomas and Y. Chao, *ACS Appl. Mater. Interfaces*, 2013, **5**, 239–242.